Int. J. Solids Structures Vol. 27, No. 7, pp. 929–945, 1991
Printed in Great Britain.

0020–7683/91 $3.00 + .00

ANALYSIS OF INTERLAMINAR STRESSES IN VISCOELASTIC COMPOSITES

KUEN Y. LIN and SUNG YI
Department of Aeronautics and Astronautics, University of Washington, Seattle, WA 98195, U.S.A.

(*Received* 20 *April* 1989; *in revised form* 6 *May* 1990)

Abstract—The viscoelastic response of laminated composites under the influence of mechanical and hygrothermal loads is studied analytically. A finite element formulation is developed for the thermo-viscoelastic solution of free edge stresses in composite laminates. Numerical results are obtained to verify the present finite element approach and to demonstrate the viscoelastic effect in graphite/epoxy composites. In addition, the effect of laminate orientations and environmental conditions on the interlaminar stress distributions and histories is presented.

1. INTRODUCTION

Laminated composites develop interlaminar stresses near a free edge due mainly to mismatches in layer properties (Pipes and Pagano, 1970; Herakovich, 1976; Wang and Crossman, 1977; Herakovich *et al.*, 1979). In many cases, these stresses, as predicted by a linear elastic analysis, are sufficiently large to cause delamination. This mechanism of failure initiation is dominated by the matrix material and has been commonly observed in quasi-static loading. As the matrix exhibits time-dependent effects, there is concern about the viscoelastic response of polymeric composites over a long time period, especially at elevated temperatures or in the presence of moisture (Crossman and Flaggs, 1979; Yeow *et al.*, 1979). Although the viscoelastic effect tends to lower the stresses in a laminate under a constant load, the situation can be quite different in the event that the applied load fluctuates with time. In this case, it has been found that the viscoelastic effect can lead to a state of stress which is higher than that obtained by an elastic analysis (Flaggs and Crossman, 1981; Weitsman, 1979). This effect would increase the probability of microcrack formation near a free edge and thus is unfavorable in consideration of environmental durability. Therefore, it is important to develop an accurate analysis method for the study of the time-dependent interlaminar stress distribution in composite laminates during their exposure to hygrothermal environments.

Analysis of the viscoelastic response of composites is complicated by their history-dependent nature. All the past responses over previous loading periods need to be accumulated in order to determine the deformation at a specific time. This complexity has limited the closed-form solution to the special case of simple laminate geometry (Chung and Bradshaw, 1981; Flaggs and Crossman, 1981; Tuttle and Brinson, 1985). Recently, Lin and Hwang developed a finite element formulation and obtained a viscoelastic solution for composite laminates with a circular hole (Lin and Hwang, 1989). This method is extended here to account for the free edge effects under the influence of mechanical and hygrothermal loads. A generalized plane strain finite element is formulated using the integral form of the constitutive equation and a variational theorem for viscoelasticity. Using this approach, the interlaminar normal and shear stress distributions near a free edge are obtained as functions of time. The effects of ply orientations and temperature/moisture conditions on the stress histories are also studied.

2. GOVERNING EQUATIONS

Consider a viscoelastic body which is very long in the x-direction, as shown in Fig. 1. It is assumed that: (1) the geometry has a constant yz cross-section and (2) mechanical and hygrothermal loads do not vary in the x-direction. Under these conditions, the resulting stresses and strains are independent of the x-coordinate and the body is in a state of

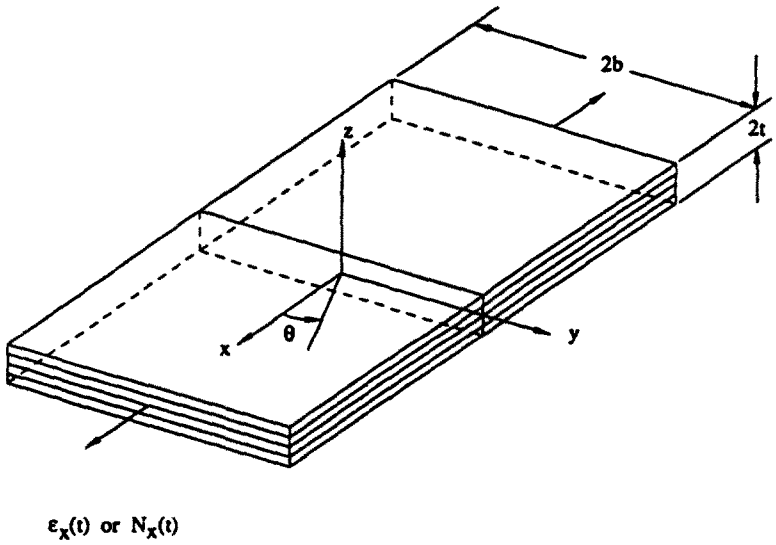

Fig. 1. Laminate geometry.

generalized plane strain. The engineering strain–displacement relationship for a viscoelastic solid in the generalized plane strain state is

$$\varepsilon_x = \frac{\partial u}{\partial x} = \varepsilon_0, \quad \varepsilon_y = \frac{\partial v}{\partial y}, \quad \varepsilon_z = \frac{\partial w}{\partial z}$$

$$\gamma_{xy} = \frac{\partial u}{\partial y}, \quad \gamma_{xz} = \frac{\partial u}{\partial z}$$

$$\gamma_{yz} = \frac{\partial v}{\partial z} + \frac{\partial w}{\partial y} \tag{1}$$

where u, v and w are displacements in the x-, y- and z-directions, respectively. The strains and displacements are functions of both position and time.

The equations of equilibrium in the absence of body forces reduce to

$$\frac{\partial \tau_{xy}}{\partial y} + \frac{\partial \tau_{xz}}{\partial z} = 0$$

$$\frac{\partial \sigma_y}{\partial y} + \frac{\partial \tau_{yz}}{\partial z} = 0$$

$$\frac{\partial \tau_{zy}}{\partial y} + \frac{\partial \sigma_z}{\partial z} = 0. \tag{2}$$

Using contracted notations for the stresses and strains, the constitutive equation for a linear anisotropic material can be expressed by the following integral (Schapery, 1967):

$$\sigma_i(T, M, t) = \int_{-\infty}^{t} C_{ij}(T, M, t-\tau) \frac{\partial}{\partial \tau} \{\varepsilon_j(\tau) - \varepsilon_j^*(\tau)\} \, d\tau \quad \text{for } i,j = 1, 2, \ldots, 6 \tag{3}$$

where σ_i is the stress component; ε_j and ε_j^* are the total engineering strain and hygrothermal strain, respectively; C_{ij} is the relaxation modulus; T is the temperature; and M is the moisture content. t denotes time and τ is a dummy variable for integration. The free hygrothermal strain ε_j^* is related to the temperature and moisture changes by

$$\varepsilon_j^* = \alpha_j \theta_T + \beta_j \theta_M$$

where α_j and β_j are coefficients of thermal and hygroscopic expansion, respectively, and θ_T and θ_M are the changes in temperature and moisture from the stress-free state. The relaxation moduli C_{ij} are determined experimentally as functions of time at various temperatures.

Using the time–temperature/moisture superposition principle, master curves for relaxation moduli can be defined as follows

$$C_{ij}(T, M, t) = C_{ij}[T_0, M_0, \zeta_{ij}(t)] \tag{4}$$

where T_0 is the reference temperature, M_0 the reference moisture, and $\zeta_{ij}(t)$ is the reduced time. The reduced time ζ_{ij}, which is related to the temperature/moisture shift factor, is defined as (Morland and Lee, 1960):

$$\zeta_{ij}(t) = \int_0^t b_{ij}(T(s), M(s))\, \mathrm{d}s \tag{5}$$

where $b_{ij}(T(s), M(s))$ is the temperature/moisture shift factor determined from the master curve of the relaxation modulus. For the case of constant temperature and moisture, eqn (5) is reduced to

$$\zeta_{ij}(t) = b_{ij}(T, M)\, t. \tag{6}$$

Substituting eqn (4) into eqn (3) yields the following constitutive relation in linear thermo-viscoelasticity:

$$\sigma_i(T, M, t) = \int_{-\infty}^{t} C_{ij}[T_0, M_0, \zeta_{ij}(t) - \zeta'_{ij}(\tau)] \frac{\partial}{\partial \tau} (\varepsilon_j(\tau) - \varepsilon_j^*(\tau))\, \mathrm{d}\tau. \tag{7}$$

For computational purposes, the relaxation moduli C_{ij} can be conveniently expressed in terms of the following exponential series

$$C_{ij}(t) = C_{ij,0} + \sum_{\omega=1}^{NT} C_{ij,\omega}\, \mathrm{e}^{-t/\lambda_{ij,\omega}} \tag{8}$$

where NT is the number of terms used in the series expansion and the constants $\lambda_{ij,\omega}$ are the relaxation times.

For a 3-D orthotropic material, the nine independent C_{ij} and the associated reduced times ζ_{ij} can be written in the following abbreviated form:

$$\begin{aligned} &C_1 = C_{11}, \quad C_2 = C_{12}, \quad C_3 = C_{13}, \ldots, C_9 = C_{66} \quad \text{and} \\ &\zeta_1 = \zeta_{11}, \quad \zeta_2 = \zeta_{12}, \ldots, \zeta_9 = \zeta_{66}, \quad \lambda_{1,\omega} = \lambda_{11,\omega}, \text{ etc.} \end{aligned} \tag{9}$$

Then the transformed $\bar{C}_{ij}$ along arbitrary coordinates in the xyz system become

$$\bar{C}_{ij}(t) = \sum_{r=1}^{9} \eta_{ij,r} \left\{ C_{r,0} + \sum_{\omega=1}^{NT} C_{r,\omega}\, \mathrm{e}^{-t/\lambda_{r,\omega}} \right\} \tag{10}$$

where $i, j = 1, 2, 3, \ldots, 6$, and $r = 1, 2, 3, \ldots, 9$. The transformation coefficients $\eta_{ij,r}$ are given in the Appendix.

In addition, the variational functional for linear thermo-viscoelastic problems can be defined as (Christensen, 1971):

$$\pi = \int_V \int_{s=-\infty}^{s=t} \int_{\tau=-\infty}^{\tau=t-s} \left\{ \tfrac{1}{2} \bar{C}_{ij}(T, M, t-s-\tau) \frac{\partial \varepsilon_i(\tau)}{\partial \tau} \frac{\partial \varepsilon_j(s)}{\partial s} - \bar{C}_{ij}(T, M, t-s-\tau) \frac{\partial \varepsilon_i^*(\tau)}{\partial \tau} \frac{\partial \varepsilon_j(s)}{\partial s} \right\} d\tau \, ds \, dV - \int_\Omega \int_{s=-\infty}^{s=t} \bar{T}_i(t-s) \frac{\partial u_i(s)}{\partial s} ds \, d\Omega \quad (11)$$

where u_i is the displacement and $\bar{T}_i$ is the prescribed surface traction on the surface Ω. The first variation of the above functional was shown to be stationary (Christensen, 1971), that is,

$$\delta\pi = \int_V \int_{s=-\infty}^{s=t} \int_{\tau=-\infty}^{\tau=t-s} \bar{C}_{ij}(T, M, t-s-\tau) \frac{\partial}{\partial \tau} \{\varepsilon_i(\tau) - \varepsilon_i^*(\tau)\} \, d\tau \frac{\partial \delta\varepsilon_j(s)}{\partial s} ds \, dV - \int_\Omega \int_{s=-\infty}^{s=t} \bar{T}_i(t-s) \frac{\partial \delta u_i(s)}{\partial s} ds \, d\Omega = 0. \quad (12)$$

3. FINITE ELEMENT FORMULATION

A special finite element will be derived for the solution of thermo-viscoelastic problems in composites. Consider the geometry of a laminate in the state of generalized plane strain, as shown in Fig. 1. The associated displacement field was shown to be (Pipes and Pagano, 1970):

$$\begin{aligned} u &= x\varepsilon_0(t) + U(y, z, t) \\ v &= V(y, z, t) \\ w &= W(y, z, t) \end{aligned} \quad (13)$$

where $\varepsilon_0(t)$ is the uniform extensional strain applied to the laminate. In the case of hygro-thermal loading, $\varepsilon_0(t)$ is the resulting laminate strain to be solved by the finite element method.

The finite element representation of the above generalized plane-strain problem consists of a cross-sectional geometry in the yz plane subdivided into a finite number of elements (Wang and Crossman, 1977). The four-noded rectangular elements incorporating three degrees of freedom (U, V, W) per node will be used for this problem. The shape functions for an element are bilinear, namely

$$\begin{Bmatrix} U(y, z, t) \\ V(y, z, t) \\ W(y, z, t) \end{Bmatrix} = [N(y, z)]\{q(t)\} \quad (14)$$

where

$$[N(y,z)] = \left[\begin{array}{ccc|ccc|ccc|ccc} N_1 & 0 & 0 & N_2 & 0 & 0 & N_3 & 0 & 0 & N_4 & 0 & 0 \\ 0 & N_1 & 0 & 0 & N_2 & 0 & 0 & N_3 & 0 & 0 & N_4 & 0 \\ 0 & 0 & N_1 & 0 & 0 & N_2 & 0 & 0 & N_3 & 0 & 0 & N_4 \end{array}\right]$$

with

$$N_1 = \left(1-\frac{y}{a}\right)\left(1-\frac{z}{b}\right), \quad N_2 = \frac{y}{a}\left(1-\frac{z}{b}\right), \quad N_3 = \frac{yz}{ab}, \quad N_4 = \frac{z}{b}\left(1-\frac{y}{a}\right)$$

and

$$\{q(t)\} = \lfloor q_1 \quad q_2 \quad q_3 \quad q_4 \quad q_5 \quad q_6 \quad q_7 \quad q_8 \quad q_9 \quad q_{10} \quad q_{11} \quad q_{12} \rfloor^T.$$

In the above, a and b are the y- and z-dimensions of the element, respectively, $N_i(y, z)$ is the bilinear shape function and $\{q(t)\}$ is the nodal displacement vector.

By substituting eqn (14) into eqn (13), the displacement field within an element can be described in terms of the assumed shape functions $\{N_i\}$, the strain ε_0, and the nodal displacement vector $\{q(t)\}$:

$$\begin{Bmatrix} u \\ v \\ w \end{Bmatrix} = \begin{Bmatrix} x\varepsilon_0(t) + U \\ V \\ W \end{Bmatrix} = [\mathbf{M} \quad \mathbf{N}] \begin{Bmatrix} \varepsilon_0(t) \\ \mathbf{q}(t) \end{Bmatrix} \tag{15}$$

where $\{M\}$ is $\lfloor x \quad 0 \quad 0 \rfloor^T$. By differentiating eqn (15) with respect to x, y and z, the following strain–displacement relationship can be obtained:

$$\{\varepsilon(t)\} = \begin{bmatrix} \mathbf{1} & \mathbf{0} \\ \mathbf{0} & \mathbf{B}(y,z) \end{bmatrix} \begin{Bmatrix} \varepsilon_0(t) \\ \mathbf{q}(t) \end{Bmatrix}. \tag{16}$$

Note that the strain vector can be partitioned as

$$\{\varepsilon(t)\} = \begin{Bmatrix} \varepsilon_0(t) \\ \varepsilon'(t) \end{Bmatrix} \tag{17}$$

where $\{\varepsilon'(t)\} = \lfloor \varepsilon_y \quad \varepsilon_z \quad \gamma_{yz} \quad \gamma_{zx} \quad \gamma_{xy} \rfloor^T$.

Substitution of eqn (15) and eqn (16) into the variational expression in eqn (12) yields the following finite element equilibrium equations for the element:

$$\int_{-\infty}^{t} k_{mn}(\zeta_r - \zeta_r') \frac{\partial q_n'(\tau)}{\partial \tau} d\tau = f_m(t) - f_m^o(t). \tag{18}$$

It is noted that $f_m^o(t)$ represents the element "residual" nodal force and $f_m(t)$ is the "reactive" nodal force which is unknown at this stage. For the mechanical loading case, $q_n'(\tau)$ becomes

$$\{q_n'(\tau)\} = \{\mathbf{q}(\tau)\}.$$

For hygrothermal loading, $q_n'(\tau)$ is expressed as

$$\{q_n'(\tau)\} = \begin{Bmatrix} \mathbf{q}(\tau) \\ \varepsilon_0(\tau) \end{Bmatrix}$$

where $\varepsilon_0(\tau)$ is the laminate hygrothermal strain to be calculated.

In the case of mechanical loading only, the element stiffness matrix $[k_{mn}]$ and the element nodal force vector $\{f_m^0\}$ can be calculated as follows:

$$k_{mn}(\zeta_r-\zeta_r') = \int\int_\Gamma B_{im}\bar{D}_{ij}(\zeta_r-\zeta_r')B_{jn}\,dy\,dz$$
$$= \sum_{r=1}^{9}\left\{k_{mnr,0}+\sum_{\omega=1}^{NT}k_{mnr,\omega}\exp[-(\zeta_r-\zeta_r')/\lambda_{r,\omega}]\right\} \tag{19}$$

and

$$f_m^0(t) = \int\int_\Gamma\int_{\tau=-\infty}^{\tau=t} B_{im}\bar{C}_{i1}(\zeta_r-\zeta_r')\frac{\partial\varepsilon_0(\tau)}{\partial\tau}d\tau\,dy\,dz$$
$$= \sum_{r=1}^{9}\left\{\left\{f_{mr,0}+\sum_{\omega=1}^{NT}f_{mr,\omega}\exp[-\zeta_r/\lambda_{r,\omega}]\right\}\varepsilon_0(0)\right.$$
$$\left.+\int_{\tau=0}^{\tau=t}\left\{f_{mr,0}+\sum_{\omega=1}^{NT}f_{mr,\omega}\exp[-(\zeta_r-\zeta_r')/\lambda_{r,\omega}]\right\}\frac{\partial\varepsilon_0(\tau)}{\partial\tau}d\tau\right\} \tag{20}$$

where $i, j = 1, 2, \ldots, 5$ and $m, n = 1, 2, \ldots, 12$. NT is the number of expanded terms used for the relaxation moduli, Γ denotes the area of the element and

$$\bar{D}_{ij}(\zeta_r-\zeta_r') = \bar{C}_{(i+1)(j+1)}(\zeta_r-\zeta_r')$$
$$k_{mnr,0} = C_{r,0}\int\int_\Gamma B_{im}\eta_{(i+1)(j+1),r}B_{jn}\,dy\,dz$$
$$k_{mnr,\omega} = C_{r,\omega}\int\int_\Gamma B_{im}\eta_{(i+1)(j+1),r}B_{jn}\,dy\,dz$$
$$f_{mr,0} = C_{r,0}\int\int_\Gamma B_{im}\eta_{i1,r}\,dy\,dz$$
$$f_{mr,\omega} = C_{r,\omega}\int\int_\Gamma B_{im}\eta_{i1,r}\,dy\,dz \tag{21}$$

(summation over repeated indices, except for r).

For hygrothermal loads, the element stiffness matrix k_{mn} is a 13×13 matrix. The 12×12 components of this matrix are shown in eqn (19). Other components are shown below:

$$k_{m,13} = \int\int_\Gamma B_{im}\bar{C}_{i1}(\zeta_r-\zeta_r')\,dy\,dz$$
$$k_{13,m} = \int\int_\Gamma \bar{C}_{1i}(\zeta_r-\zeta_r')B_{im}\,dy\,dz$$
$$k_{13,13} = \int\int_\Gamma \bar{C}_{11}(\zeta_r-\zeta_r')\,dy\,dz$$
$$(i, j = 1, 2, \ldots, 5). \tag{22}$$

Similar to the mechanical load case, the element stiffness matrix associated with hygrothermal loading can be expressed as

$$k_{mn}(\zeta_r-\zeta_r') = \sum_{r=1}^{9}\left\{k_{mnr,0}+\sum_{\omega=1}^{NT}k_{mnr,\omega}\exp[-(\zeta_r-\zeta_r')/\lambda_{r,\omega}]\right\} \tag{23}$$

where $m, n = 1, 2, \ldots, 13$.

The residual nodal force vector due to hygrothermal loads becomes

$$\{f_m^n(t)\} = -\int\int_{\Gamma}\int_{\tau=-\infty}^{\tau=t}\left\{B_{im}\bar{D}_{ij}(\zeta_r-\zeta_r')\frac{\partial\varepsilon_{(j+1)}^*(\tau)}{\partial\tau}+B_{im}\bar{C}_{i1}(\zeta_r-\zeta_r')\frac{\partial\varepsilon_1^*(\tau)}{\partial\tau}\right\}d\tau\,dy\,dz \tag{24}$$

and

$$f_{13}^n(t) = -\int\int_{\Gamma}\int_{\tau=-\infty}^{\tau=t}\left\{\bar{C}_{1i}(\zeta_r-\zeta_r')\frac{\partial\varepsilon_{(j+1)}^*(\tau)}{\partial\tau}+\bar{C}_{11}(\zeta_r-\zeta_r')\frac{\partial\varepsilon_1^*(\tau)}{\partial\tau}\right\}d\tau\,dy\,dz$$

where $i,j = 1,2,\ldots,5$, $m = 1,2,\ldots,12$, and

$$\{\varepsilon^*(\tau)\} = \lfloor\varepsilon_x^*\quad\varepsilon_y^*\quad\varepsilon_z^*\quad\varepsilon_{yz}^*\quad\varepsilon_{zx}^*\quad\varepsilon_{xy}^*\rfloor^T. \tag{25}$$

Using the exponential series for C_{ij}, as given in eqn (10), the following force vector can be derived

$$\begin{aligned}f_m^n(t) = -\sum_{r=1}^{9}\Bigg\{&\left\{f_{mr,0}^{\alpha}+\sum_{\omega=1}^{NT}f_{mr,\omega}^{\alpha}\exp[-\zeta_r/\lambda_{r,\omega}]\right\}\theta_T(0)\\&+\left\{f_{mr,0}^{\beta}+\sum_{\omega=1}^{NT}f_{mr,\omega}^{\beta}\exp[-\zeta_r/\lambda_{r,\omega}]\right\}\theta_M(0)\\&+\int_{\tau=0}^{\tau=t}\Bigg\{\left\{f_{mr,0}^{\alpha}+\sum_{\omega=1}^{NT}f_{mr,\omega}^{\alpha}\exp[-(\zeta_r-\zeta_r')/\lambda_{r,\omega}]\right\}\frac{\partial\theta_T(\tau)}{\partial\tau}\\&+\left\{f_{mr,0}^{\beta}+\sum_{\omega=1}^{NT}f_{mr,\omega}^{\beta}\exp[-(\zeta_r-\zeta_r')/\lambda_{r,\omega}]\right\}\frac{\partial\theta_M(\tau)}{\partial\tau}\Bigg\}d\tau\Bigg\}\end{aligned} \tag{26}$$

where $m = 1,2,3,\ldots,12$ and

$$\begin{aligned}f_{13}^n(t) = -\sum_{r=1}^{9}\Bigg\{&\left\{f_{13r,0}^{\alpha}+\sum_{\omega=1}^{NT}f_{13r,\omega}^{\alpha}\exp[-\zeta_r/\lambda_{r,\omega}]\right\}\theta_T(0)\\&+\left\{f_{13r,0}^{\beta}+\sum_{\omega=1}^{NT}f_{13r,\omega}^{\beta}\exp[-\zeta_r/\lambda_{r,\omega}]\right\}\theta_M(0)\\&+\int_{\tau=0}^{\tau=t}\Bigg\{\left\{f_{13r,0}^{\alpha}+\sum_{\omega=1}^{NT}f_{13r,\omega}^{\alpha}\exp[-(\zeta_r-\zeta_r')/\lambda_{r,\omega}]\right\}\frac{\partial\theta_T(\tau)}{\partial\tau}\\&+\left\{f_{13r,0}^{\beta}+\sum_{\omega=1}^{NT}f_{13r,\omega}^{\beta}\exp[-(\zeta_r-\zeta_r')/\lambda_{r,\omega}]\right\}\frac{\partial\theta_M(\tau)}{\partial\tau}\Bigg\}d\tau\Bigg\}\end{aligned}$$

where

$$f^{\alpha}_{mr,\omega} = C_{r,\omega}\int\int_{\Gamma}\{B_{im}\eta_{(i+1)(j+1),r}\bar{\alpha}_{(j+1)} + B_{im}\eta_{i1,r}\bar{\alpha}_1\}\,dy\,dz$$

$$f^{\beta}_{mr,\omega} = C_{r,\omega}\int\int_{\Gamma}\{B_{im}\eta_{(i+1)(j+1),r}\bar{\beta}_{(j+1)} + B_{im}\eta_{i1,r}\bar{\beta}_1\}\,dy\,dz$$

$$f^{\alpha}_{13r,\omega} = C_{r,\omega}\int\int_{\Gamma}\{\eta_{1i,r}\bar{\alpha}_{(i+1)} + \eta_{11,r}\bar{\alpha}_1\}\,dy\,dz$$

$$f^{\beta}_{13r,\omega} = C_{r,\omega}\int\int_{\Gamma}\{\eta_{1i,r}\bar{\beta}_{(i+1)} + \eta_{11,r}\bar{\beta}_1\}\,dy\,dz. \tag{27}$$

Note that in the above, $i,j = 1,2,\ldots,5$, $m = 1,2,\ldots,12$, and that $\{\bar{\alpha}\}$ and $\{\bar{\beta}\}$ are the transformed coefficients of thermal and hygroscopic expansion with respect to the xyz coordinate system.

Assembly of element equations over the entire domain leads to the following global equations:

$$\int_{\tau=-\infty}^{\tau=t} K_{mn}(\zeta_r - \zeta_r')\frac{\partial u_n(\tau)}{\partial\tau}d\tau = F_m(t) - F_m^v(t) \tag{28}$$

where m, n range from 1 to the total degrees of freedom. K_{mn} is the structural (global) stiffness matrix and F_m and F_m^v are global force vectors. Note that $F_m(t)$ becomes zero if only ε_0 is applied.

4. NUMERICAL PROCEDURES

A direct integration of eqn (28) would require enormous computing time and memory storage since the stiffness matrix is history-dependent. To overcome these difficulties, the numerical algorithm derived by Taylor *et al.* (1970) for isotropic materials is extended here for the solution of eqn (28). In this procedure, the derivative of displacement u_n with respect to time is approximated by

$$\frac{\partial u_n(t)}{\partial t} \simeq \frac{\Delta u_n(t_j)}{\Delta t_j} \equiv \frac{u_n(t_j) - u_n(t_{j-1})}{t_j - t_{j-1}}, \quad t_{j-1} \leqslant t \leqslant t_j. \tag{29}$$

It is assumed that both mechanical and hygrothermal loads are linear during each time interval, i.e.

$$\frac{\partial\varepsilon_0(t)}{\partial t} \simeq \frac{\Delta\varepsilon_0(t_j)}{\Delta t_j} = \frac{\varepsilon_0(t_j) - \varepsilon_0(t_{j-1})}{\Delta t_j}$$

$$\frac{\partial\theta_T(t)}{\partial t} \simeq \frac{\Delta\theta_T(t_j)}{\Delta t_j} = \frac{\theta_T(t_j) - \theta_T(t_{j-1})}{\Delta t_j}$$

$$\frac{\partial\theta_M(t)}{\partial t} \simeq \frac{\Delta\theta_M(t_j)}{\Delta t_j} = \frac{\theta_M(t_j) - \theta_M(t_{j-1})}{\Delta t_j}. \tag{30}$$

Assuming that there is no loading applied at time $t < 0$, the initial values for the strain, temperature, and moisture differences are

$$\Delta\varepsilon_0(0) = \varepsilon_0(0)$$

$$\Delta\theta_T(0) = \theta_T(0)$$

$$\Delta\theta_M(0) = \theta_M(0). \tag{31}$$

Using the approximations for displacements and loads in eqns (29) and (30), eqn (28) can be expressed in a recursive form

$$\sum_{r=1}^{9}\left\{K_{mnr,0}+\sum_{\omega=1}^{NT}K_{mnr,\omega}H_{r,\omega}(\Delta t_p)\right\}\Delta u_n(t_p)$$
$$=F_m(t_p)-F'_m(t_p)-\sum_{r=1}^{9}\left\{K_{mnr,0}u_n(t_{p-1})+\sum_{\omega=1}^{NT}\bar{G}_{mr,\omega}(t_p)\right\} \quad (32)$$

in which $K_{mnr,0}$ and $K_{mnr,\omega}$ denote the global matrices as assembled from the element matrices of $k_{mnr,0}$ and $k_{mnr,\omega}$ in eqn (19) or eqn (23). In the case of mechanical loading, F'_m and $\bar{G}_{mr,\omega}$ are given by

$$F'_m(t_p)=\sum_{r=1}^{9}\left\{F_{mr,0}\varepsilon_0(t_p)+\sum_{\omega=1}^{NT}F_{mr,\omega}\Delta\varepsilon_0(t_p)H_{r,\omega}(\Delta t_p)\right\} \quad (33)$$

and

$$\bar{G}_{mr,\omega}(t_p)=\exp(-\Delta\zeta_{r,t_p}/\lambda_{r,\omega})\{\bar{G}_{mr,\omega}(t_{p-1})+[K_{mnr,\omega}\Delta u_n(t_{p-1})$$
$$+F_{mr,\omega}\Delta\varepsilon_0(t_{p-1})]H_{r,\omega}(\Delta t_{p-1})\} \quad (34)$$

with

$$\bar{G}_{mr,\omega}(0)=0$$
$$H_{r,\omega}(\Delta t_p)=\frac{1}{\Delta t_p}\int_{t_{p-1}}^{t_p}\exp[-(\Delta\zeta_{r,t_p})/\lambda_{r,\omega}]\,d\tau$$
$$H_{r,\omega}(0)=1$$
$$\zeta_{r,t_p}=\zeta_r(t_p)$$
$$\Delta\zeta_{r,t_p}=\zeta_{r,t_p}-\zeta_{r,t_{p-1}}. \quad (35)$$

For the hygrothermal loading case, F'_m and $\bar{G}_{mr,\omega}$ are defined as follows:

$$F'_m(t_p)=-\sum_{r=1}^{9}\left[F^{\alpha}_{mr,0}\theta_T(t_p)+F^{\beta}_{mr,0}\theta_M(t_p)\right.$$
$$\left.+\sum_{\omega=1}^{NT}\{F^{\alpha}_{mr,\omega}\Delta\theta_T(t_p)+F^{\beta}_{mr,0}\Delta\theta_M(t_p)\}H_{r,\omega}(\Delta t_p)\right] \quad (36)$$

and

$$\bar{G}_{mr,\omega}(t_p)=\exp(-\Delta\zeta_{r,t_p}/\lambda_{r,\omega})\{\bar{G}_{mr,\omega}(t_{p-1})+[K_{mnr,\omega}\Delta u_n(t_{p-1})$$
$$-F^{\alpha}_{mr,\omega}\Delta\theta_T(t_{p-1})-F^{\beta}_{mr,\omega}\Delta\theta_M(t_{p-1})]H_{r,\omega}(\Delta t_{p-1})\}. \quad (37)$$

Note that eqn (32) is in a recursive form. Therefore it is possible to solve for the displacements u_n at time t_p using only the previous solution at time t_{p-1}. Similarly, employing the transformed constitutive equations of eqn (7), in the xyz coordinate system, the stress component within an element can be described by the recursive equation:

$$\sigma_i(t_p) = \sum_{r=1}^{9} \left\{ C_{r,0}\eta_{ij,r}\{\varepsilon_j(t_p) - \bar{\alpha}_j\theta_T(t_p) - \bar{\beta}_j\theta_M(t_p)\} + \sum_{\omega=1}^{NT} [C_{r,\omega}\eta_{ij,r}H_{r,\omega}(\Delta t_p)\{\Delta\varepsilon_j(t_p) - \bar{\alpha}_j\Delta\theta_T(t_p) - \bar{\beta}_j\Delta\theta_M(t_p)\} + G^s_{ir,\omega}(t_p)] \right\} \quad (38)$$

where $i, j = 1, 2, \ldots, 6$ (summation over j) and

$$G^s_{ir,\omega}(t_p) = \exp(-\Delta\zeta_{r,t_p}/\lambda_{r,\omega})[G^s_{ir,\omega}(t_{p-1}) + C_{r,\omega}\eta_{ij,r}H_{r,\omega}(\Delta t_{p-1}) \cdot \{\Delta\varepsilon_j(t_{p-1}) - \bar{\alpha}_j\Delta\theta_T(t_{p-1}) - \bar{\beta}_j\Delta\theta_M(t_{p-1})\}]. \quad (39)$$

After the $\Delta u_n(t_p)$ are obtained from eqn (32), the displacements $u_n(t_p)$ can be found from eqn (29). The strain field is then obtained from the strain–displacement relations in eqn (16). Finally, the stresses can be computed from the constitutive equations in eqn (38).

5. RESULTS FOR INTERLAMINAR STRESSES

Based on the preceding formulation, numerical results have been obtained for the time-dependent interlaminar stresses in graphite/epoxy composites subjected to mechanical and hygrothermal loads. The elastic material properties, master relaxation modulus curves and the shift factors corresponding to various moisture contents and temperatures were investigated by Crossman *et al.* (1978) and these values are used in the present study. It is assumed that E_3 of the lamina is equal to E_2 and $G_{12} = G_{13} = G_{23}$. Also, Poisson's ratios ν_{23} and ν_{13} are assumed to be the same as ν_{12}. Since E_1 is in general dominated by fiber properties, it is assumed that stiffness C_{11} is time-independent while other relaxation moduli such as C_{12}, C_{13}, C_{22}, C_{23}, C_{33}, C_{44}, C_{55} and C_{66} have the same time-dependent function.

Using the reduced time associated with the temperature/moisture shift factors, the variation of material properties C_{ij} at various temperatures can be found. Figure 2 shows the C_{66} values as a function of time at $T = 77°$, 122° and 140°F for the case of constant

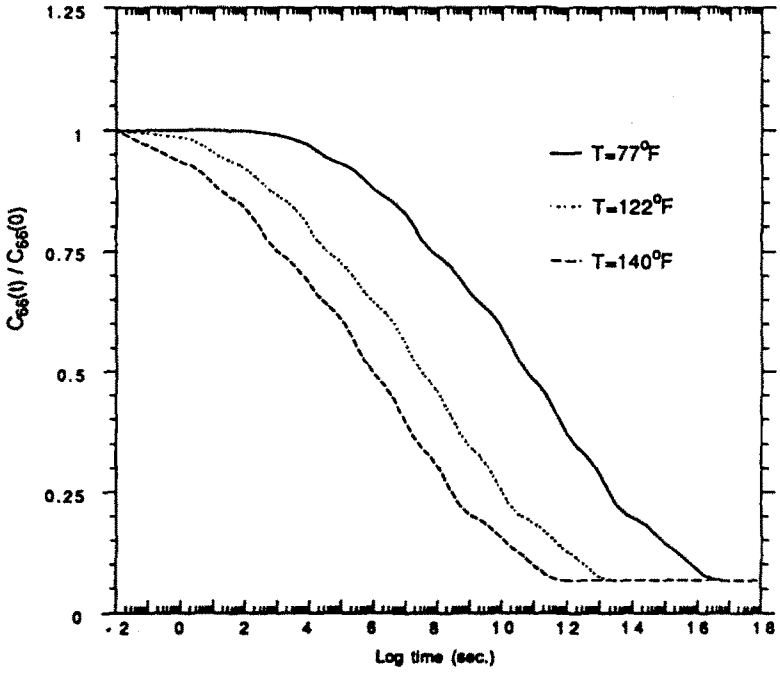

Fig. 2. Time variation of relaxation modulus at various temperatures.

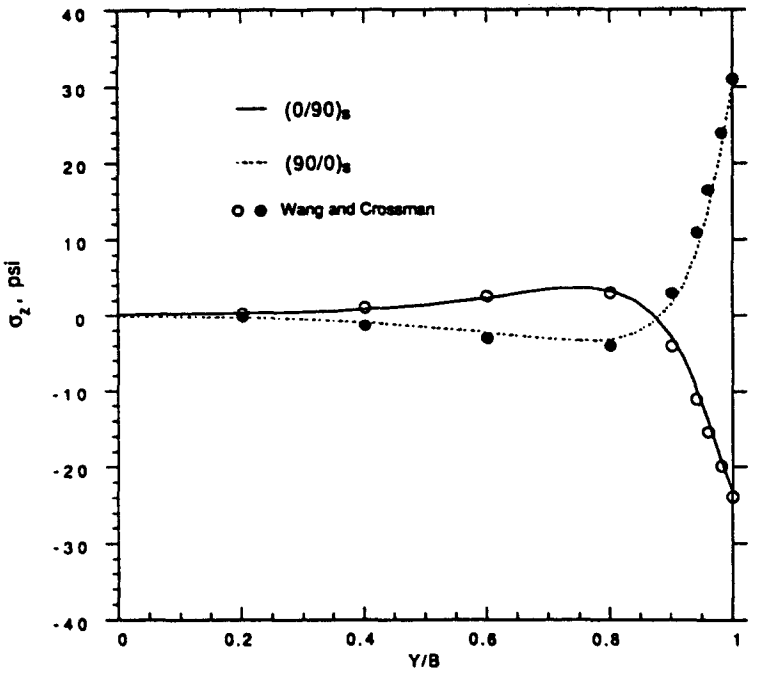

Fig. 3. Interlaminar normal stresses in cross-ply laminates ($z = 0$ in., $\Delta T = 1°F$).

moisture content ($M = 0.3\%$). It is noted that C_{66} degrades faster at high temperatures than at low temperatures.

5.1. *Comparison studies*

Since there are no solutions available on interlaminar stress histories for comparison, verification of the present approach will be limited to two special cases; an elastic solution for interlaminar stresses at $t = 0$ and a viscoelastic solution for in-plane stresses as a function of time. In the elastic case, $[0/90]_s$ and $[90/0]_s$ graphite/epoxy laminates subjected to thermal loads were considered. The resulting interlaminar stress σ_z at the mid-plane is shown in Fig. 3. Good agreement between the present solution and Wang and Crossman (1977) is observed.

In the viscoelastic case, inplane shear stress τ_{xy} in a $[\pm 45]_s$ laminate due to uniform temperature $\Delta T = 71°F$ was obtained. This solution was compared with the classical lamination solution for an infinite plate by Flaggs and Crossman (1981), as shown in Table 1. The discrepancy between these two solutions is in the range 0.9–5.6%. The differences may be attributable to the finite width (b/t) effects which are not considered by Flaggs and Crossman (1981).

5.2. *Interlaminar stress histories*

To demonstrate the present numerical procedure, the interlaminar stresses in $[0/90]_s$, $[90/0]_s$ and $[45/-45]_s$ graphite/epoxy laminates are presented. In each case, a laminate

Table 1. Viscoelastic shear stress τ_{xy} in $[\pm 45]_s$ GY70/339 composites ($\Delta T = -71°F$ and $M = 0\%$)

Time (s)	Flaggs and Crossman (1981)	Present solution	Error (%)
$t = 0$	870	877.4	0.9
$t = 1800$	762	807.3	5.6
$t = 180{,}000$	670	695.5	3.8
$t = 360{,}000$	650	667.7	2.7

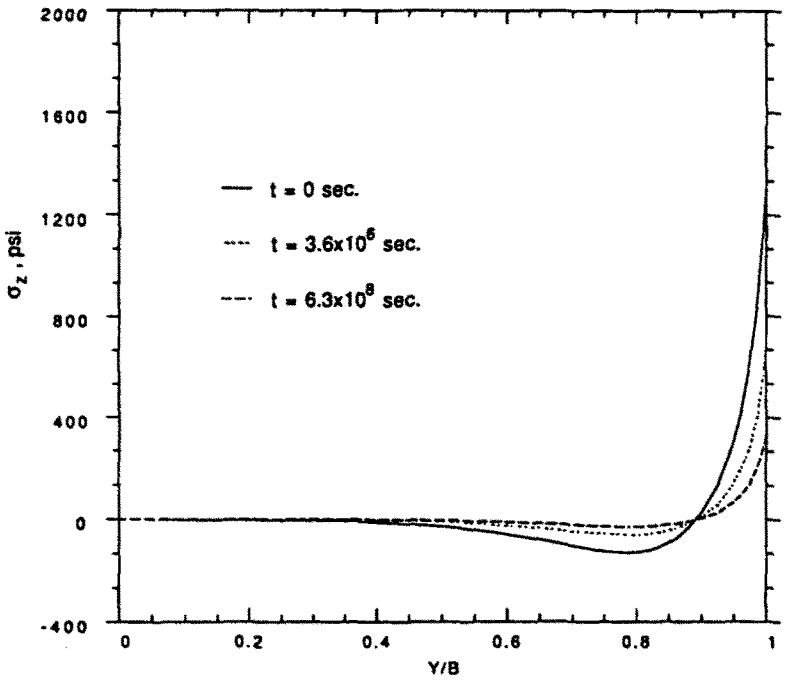

Fig. 4. Interlaminar normal stresses in a (0/90), laminate ($z = 0.0056$ in., $T = 140$°F, $M = 0.3\%$).

width-to-thickness ratio (b/t) of four is considered. The finite element model used consists of a 32×8 mesh pattern (256 elements) in the yz cross-section with a total of 891 degrees of freedom. The step size Δt is set to 200 s initially and then is allowed to increase with time to a maximum of 3×10^7 s. There are 60 time steps involved in the calculation of viscoelastic interlaminar stresses over a period of 20 years.

A uniform axial strain of $\varepsilon_x = 0.005$ in./in. is applied to the $[0/90]_s$ laminate in the 0.3% moisture environment. The resulting σ_z along the interface between the 0° and 90° layers is shown in Fig. 4 for $T = 140$°F. The results show that at $y/b \simeq 0.9$, $z = 0.0056$, σ_z seems to be independent of time. Also, it is apparent that the stress field is singular at the free edge. The order of stress singularity appears to be changing with time as can be seen from Fig. 4. Figure 5 shows the interlaminar stress history $\sigma_z(t)$ near the free edge ($y/b = 0.99$). These results have been normalized with respect to the initial stress at $t = 0$. It is seen that the rate of stress relaxation is greater at 140°F (about 75%) than at 77°F (about 32%) after $t = 10^{8.8}$ s (20 years) because material properties decrease faster at $T = 140$°F than at $T = 77$°F. At $T = 140$°F, the inplane stresses σ_x in each layer of a $(0/90)_s$ laminate are plotted in Fig. 6. Over a period of 20 years the stress σ_x relaxes about 78% in the 90° layer while σ_x remains constant in the 0° ply since C_{11} is assumed to be time-independent. The high relaxation rate is due to the fact that the GY70/339 material used in the analysis has strong time-dependent properties.

In the $[90/0]_s$ laminate, the same loading condition, $\varepsilon_x = 0.005$ in./in., is applied at $T = 140$°F and $M = 0.3\%$. The results of the interlaminar normal stress at $z = 0.0056$ in. and $z = 0.0$ in. are shown in Figs 7 and 8, respectively. Note that σ_z relaxes as time increases. In addition, while the rate of relaxation varies from point to point at each instant, σ_z is distributed in such a manner that the equilibrium condition of forces in the z-direction is satisfied.

In a $[45/-45]_s$ laminate, both σ_z and τ_{xz} are present near the free edge. For a uniform applied strain of $\varepsilon_x = 0.005$ in./in., the resulting interlaminar stress τ_{xz} is shown in Fig. 9. The distribution of σ_z along $z = 0.0056$ in. as a function of time is illustrated in Fig. 10. Near the free edge of the 45° and −45° ply interface, the magnitude of τ_{xz} is reduced by about 79% during a 20-year period. In comparison, the stress σ_z relaxes about 70% at the same location for the same period.

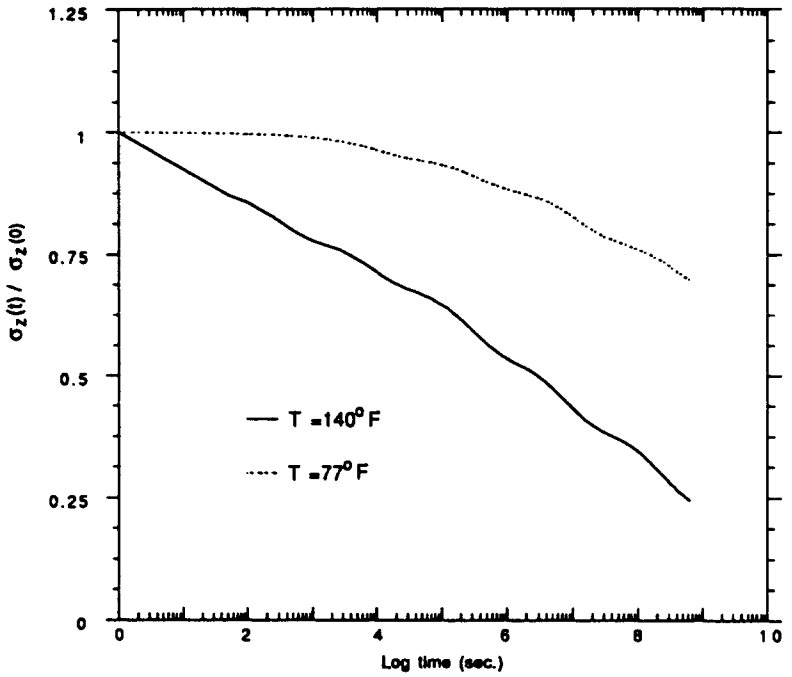

Fig. 5. Histories of interlaminar stresses at the free edge in a (0/90), laminate ($z = 0.0056$ in.).

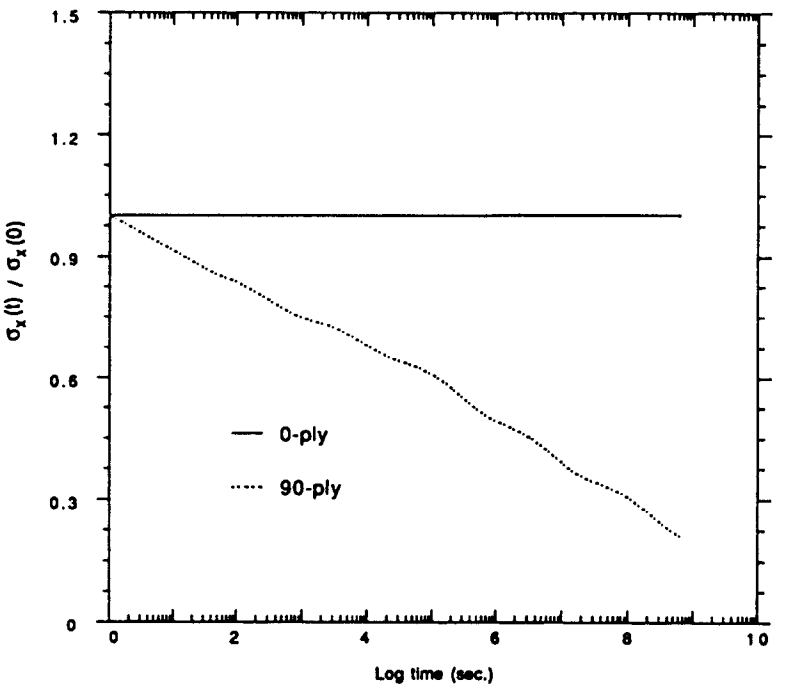

Fig. 6. In-plane stresses in 0° and 90° layers of a (0/90), laminate ($T = 140$ F, $M = 0.3\%$).

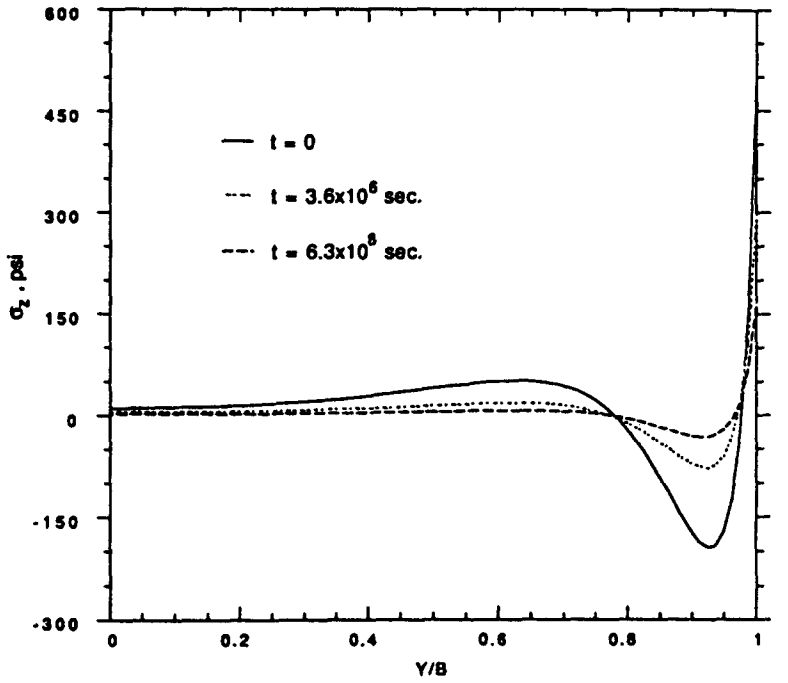

Fig. 7. Interlaminar normal stresses in a (90/0), laminate (z = 0.0056 in.).

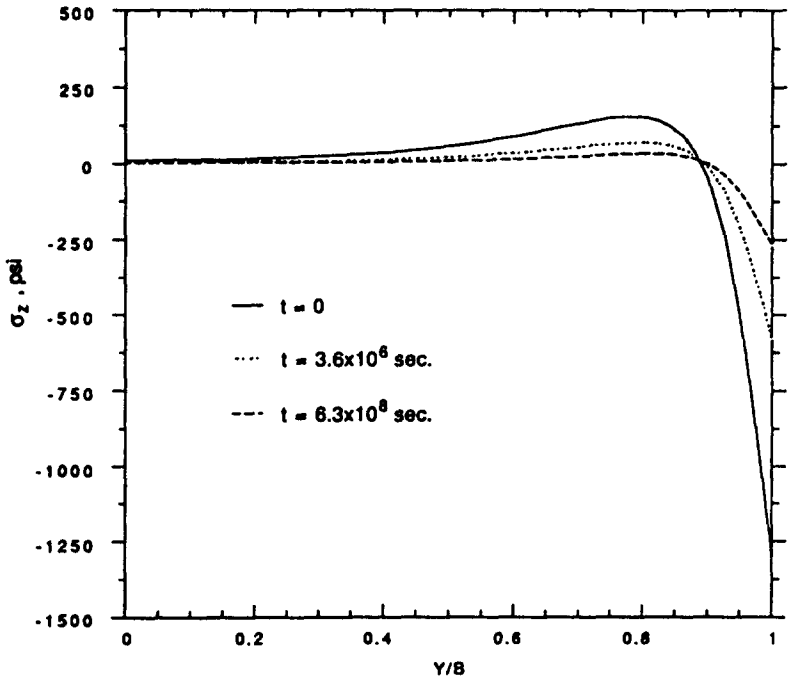

Fig. 8. Interlaminar normal stresses in a (90/0), laminate (z = 0.0 in.).

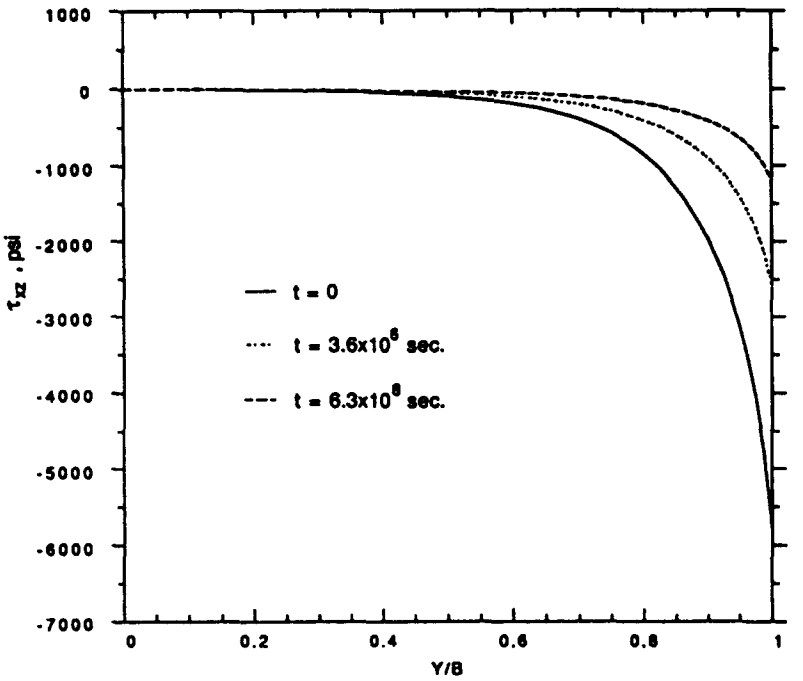

Fig. 9. Interlaminar shear stresses in a (45/−45), laminate (z = 0.0056 in., T = 140°F, M = 0.3%).

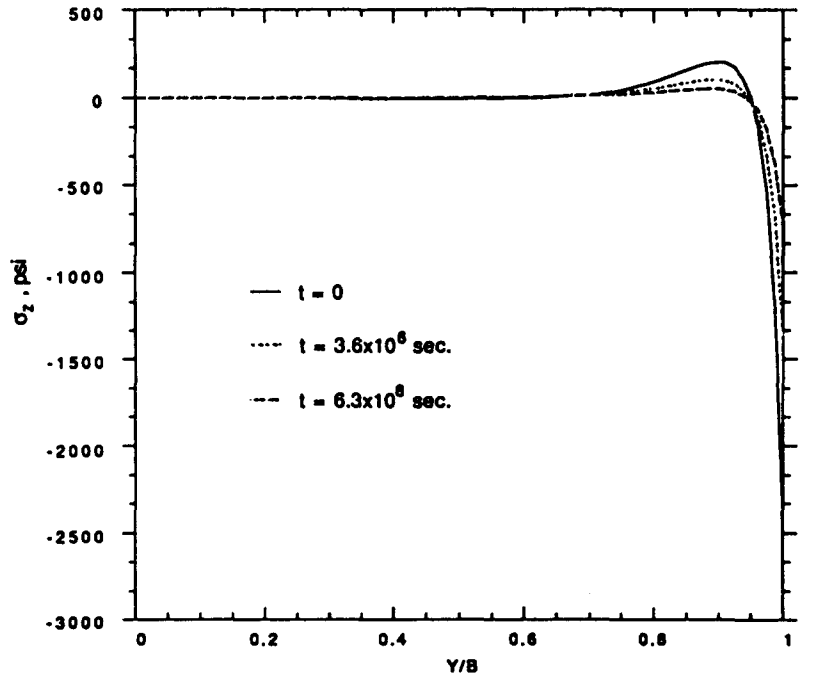

Fig. 10. Interlaminar normal stresses in a (45/−45), laminate (z = 0.0056 in.).

6. CONCLUSION

A finite element procedure has been presented for the viscoelastic solution of interlaminar stresses near a free edge in laminated composites subjected to mechanical and hygrothermal loads. Numerical results have been obtained to demonstrate the viscoelastic effect in several different laminates. These results show that both the interlaminar normal and shear stresses relax significantly when a laminate is subjected to constant strain loading. The amount of stress relaxation depends strongly upon ply orientations and hygrothermal environments. Such a time-dependent effect is important in the case of cyclic loading and must be considered in predicting the long-term response of composites at elevated environmental conditions.

REFERENCES

Christensen, R. M. (1971). *Theory of Viscoelasticity*. Academic Press, New York.

Chung, T. J. and Bradshaw, R. L. (1981). Effects of temperature and moisture on anisotropic structures. AIAA Paper No. 81-0545, 166–175.

Crossman, F. W. and Flaggs, D. L. (1979). Dimensional stability of composite laminates during environmental exposure. *SAMPE JI* 15(4), 15–20.

Crossman, F. W., Mauri, R. E. and Warren, W. J. (1978). Moisture altered viscoelastic response of graphite/epoxy composite. *Advanced composite materials—environmental effects*, ASTM STP 658 (Edited by J. R. Vinson), pp. 205–220. American Society for Testing and Materials, Philadelphia, PA.

Flaggs, D. L. and Crossman, F. W. (1981). Analysis of the viscoelastic response of composite laminates during hygrothermal exposure. *J. Composite Mater.* **15**, 21–40.

Herakovich, C. T. (1976). On thermal edge effects in composite laminates. *Int. J. Mech. Sci.* **18**(3), 129–134.

Herakovich, C. T., Nagarkar, A. and O'Brien, D. A. (1979). Failure analysis of composite laminates with free edges. In *Modern Developments in Composite Materials and Structures* (Edited by J. R. Vinson). American Society of Mechanical Engineers, New York.

Lin, K. Y. and Hwang, I. H. (1989). Thermo-viscoelastic analysis of composite materials. *J. Composite Mater.* **23**(6), 554–569.

Morland, L. W. and Lee, E. H. (1960). Stress analysis for linear viscoelastic materials with temperature variation. *Trans. Soc. Rheol.* **4**, 233–263.

Pipes, R. B. and Pagano, N. J. (1970). Interlaminar stresses in composite laminates under uniform axial extension. *J. Composite Mater.* **4**(4), 538–548.

Schapery, R. A. (1967). Stress analysis of viscoelastic composite materials. *J. Composite Mater.* **1**(3), 228–267.

Taylor, R. L., Pister, K. S. and Goudreau, G. L. (1970). Thermomechanical analysis of viscoelastic solids. *Int. J. Numer. Meth. Engng.* **2**, 45–59.

Tuttle, M. E. and Brinson, H. F. (1985). Accelerated viscoelastic characterization of T300/5208 graphite-epoxy laminates. NASA Contractor Report No. 3871.

Wang, A. S. D. and Crossman, F. W. (1977). Edge effects on thermally induced stresses in composite laminates. *J. Composite Mater.* **11**(3), 300–312.

Weitsman, Y. (1979). Residual thermal stresses due to cool-down of epoxy-resin composites. *J. Appl. Mech.* **46**, 563–567.

Yeow, Y. T., Morris, D. H. and Brinson, H. F. (1979). Time-temperature behavior of a unidirectional graphite–epoxy composite. In *Composite Materials: Testing and Design (Fifth Conf.)*, ASTM STP 674 (Edited by S. W. Tsai), pp. 263–281. American Society for Testing and Materials, Philadelphia, PA.

APPENDIX: THE TRANSFORMATION COEFFICIENTS $\eta_{ij,r}$

$$[\eta_{ij,1}] = \begin{bmatrix} m^4 & m^2n^2 & 0 & 0 & 0 & m^3n \\ m^2n^2 & n^4 & 0 & 0 & 0 & mn^3 \\ 0 & 0 & 0 & 0 & 0 & 0 \\ 0 & 0 & 0 & 0 & 0 & 0 \\ 0 & 0 & 0 & 0 & 0 & 0 \\ m^3n & mn^3 & 0 & 0 & 0 & m^2n^2 \end{bmatrix}$$

$$[\eta_{ij,2}] = \begin{bmatrix} 2m^2n^2 & m^4+n^4 & 0 & 0 & 0 & -mn(m^2-n^2) \\ m^4+n^4 & 2m^2n^2 & 0 & 0 & 0 & mn(m^2-n^2) \\ 0 & 0 & 0 & 0 & 0 & 0 \\ 0 & 0 & 0 & 0 & 0 & 0 \\ 0 & 0 & 0 & 0 & 0 & 0 \\ -mn(m^2-n^2) & mn(m^2-n^2) & 0 & 0 & 0 & -2m^2n^2 \end{bmatrix}$$

$$[\eta_{ij,3}] = \begin{bmatrix} 0 & 0 & m^2 & 0 & 0 & 0 \\ 0 & 0 & n^2 & 0 & 0 & 0 \\ m^2 & n^2 & 0 & 0 & 0 & mn \\ 0 & 0 & 0 & 0 & 0 & 0 \\ 0 & 0 & 0 & 0 & 0 & 0 \\ 0 & 0 & mn & 0 & 0 & 0 \end{bmatrix}$$

$$[\eta_{ij,4}] = \begin{bmatrix} n^4 & m^2n^2 & 0 & 0 & 0 & -mn^3 \\ m^2n^2 & m^4 & 0 & 0 & 0 & -m^3n \\ 0 & 0 & 0 & 0 & 0 & 0 \\ 0 & 0 & 0 & 0 & 0 & 0 \\ 0 & 0 & 0 & 0 & 0 & 0 \\ -mn^3 & -m^3n & 0 & 0 & 0 & m^2n^2 \end{bmatrix}$$

$$[\eta_{ij,5}] = \begin{bmatrix} 0 & 0 & n^2 & 0 & 0 & 0 \\ 0 & 0 & m^2 & 0 & 0 & 0 \\ n^2 & m^2 & 0 & 0 & 0 & -mn \\ 0 & 0 & 0 & 0 & 0 & 0 \\ 0 & 0 & 0 & 0 & 0 & 0 \\ 0 & 0 & -mn & 0 & 0 & 0 \end{bmatrix}$$

$$[\eta_{ij,6}] = \begin{bmatrix} 0 & 0 & 0 & 0 & 0 & 0 \\ 0 & 0 & 0 & 0 & 0 & 0 \\ 0 & 0 & 1 & 0 & 0 & 0 \\ 0 & 0 & 0 & 0 & 0 & 0 \\ 0 & 0 & 0 & 0 & 0 & 0 \\ 0 & 0 & 0 & 0 & 0 & 0 \end{bmatrix}$$

$$[\eta_{ij,7}] = \begin{bmatrix} 0 & 0 & 0 & 0 & 0 & 0 \\ 0 & 0 & 0 & 0 & 0 & 0 \\ 0 & 0 & 0 & 0 & 0 & 0 \\ 0 & 0 & 0 & m^2 & -mn & 0 \\ 0 & 0 & 0 & -mn & n^2 & 0 \\ 0 & 0 & 0 & 0 & 0 & 0 \end{bmatrix}$$

$$[\eta_{ij,8}] = \begin{bmatrix} 0 & 0 & 0 & 0 & 0 & 0 \\ 0 & 0 & 0 & 0 & 0 & 0 \\ 0 & 0 & 0 & 0 & 0 & 0 \\ 0 & 0 & 0 & n^2 & mn & 0 \\ 0 & 0 & 0 & mn & m^2 & 0 \\ 0 & 0 & 0 & 0 & 0 & 0 \end{bmatrix}$$

$$[\eta_{ij,9}] = \begin{bmatrix} 4m^2n^2 & -4m^2n^2 & 0 & 0 & 0 & -2mn(m^2-n^2) \\ -4m^2n^2 & 4m^2n^2 & 0 & 0 & 0 & 2mn(m^2-n^2) \\ 0 & 0 & 0 & 0 & 0 & 0 \\ 0 & 0 & 0 & 0 & 0 & 0 \\ 0 & 0 & 0 & 0 & 0 & 0 \\ -2mn(m^2-n^2) & 2mn(m^2-n^2) & 0 & 0 & 0 & (m^2-n^2)^2 \end{bmatrix}$$

where $m = \cos\theta$, $n = \sin\theta$.